Hindawi
Advances in Materials Science and Engineering
Volume 2023, Article ID 9803865, 1 page
https://doi.org/10.1155/2023/9803865

Retraction

Retracted: Synthesis, Mechanical, and Tribological Performance Analysis of Stir-Casted AA7079: $ZrO_2 + Si_3N_4$ Hybrid Composites by Taguchi Route

Advances in Materials Science and Engineering

Received 26 December 2023; Accepted 26 December 2023; Published 29 December 2023

This article has been retracted by Hindawi, as publisher, following an investigation undertaken by the publisher [1]. This investigation has uncovered evidence of systematic manipulation of the publication and peer-review process. We cannot, therefore, vouch for the reliability or integrity of this article.

Please note that this notice is intended solely to alert readers that the peer-review process of this article has been compromised.

Wiley and Hindawi regret that the usual quality checks did not identify these issues before publication and have since put additional measures in place to safeguard research integrity.

We wish to credit our Research Integrity and Research Publishing teams and anonymous and named external researchers and research integrity experts for contributing to this investigation.

The corresponding author, as the representative of all authors, has been given the opportunity to register their agreement or disagreement to this retraction. We have kept a record of any response received.

References

[1] G. Jegan, P. Kavipriya, T. Sathish, S. Dinesh Kumar, T. Samraj Lawrence, and T. Vino, "Synthesis, Mechanical, and Tribological Performance Analysis of Stir-Casted AA7079: $ZrO_2 + Si_3N_4$ Hybrid Composites by Taguchi Route," *Advances in Materials Science and Engineering*, vol. 2021, Article ID 7722370, 15 pages, 2021.

Hindawi
Advances in Materials Science and Engineering
Volume 2021, Article ID 7722370, 15 pages
https://doi.org/10.1155/2021/7722370

Research Article

Synthesis, Mechanical, and Tribological Performance Analysis of Stir-Casted AA7079: $ZrO_2 + Si_3N_4$ Hybrid Composites by Taguchi Route

G. Jegan,[1] P. Kavipriya,[1] T. Sathish,[2] S. Dinesh Kumar,[3] T. Samraj Lawrence ,[4] and T. Vino[1]

[1]*Department of Electronics and Communication Engineering, Sathyabama Institute of Science and Technology, Chennai 600 119, Tamil Nadu, India*
[2]*Department of Mechanical Engineering, Saveetha School of Engineering, SIMATS, Chennai 600 125, Tamil Nadu, India*
[3]*Department of Mechanical Engineering, St. Peter's Institute of Higher Education and Research, Avadi, Chennai 600 054, Tamil Nadu, India*
[4]*Department of Information Technology, College of Engineering and Technology, Dambi Dollo University, Dambi Dollo, Oromia Region, Ethiopia*

Correspondence should be addressed to T. Samraj Lawrence; samrajlawrencet@gmail.com

Received 24 May 2021; Accepted 8 June 2021; Published 19 June 2021

Academic Editor: Samson Jerold Samuel Chelladurai

Currently, the aluminum alloys are utilized more in level of all industries for different applications; furthermore, industries need high-strength alloys for making innovative components. For those reasons, many researchers hope to prepare hybrid aluminum metal matrix composites at various composition levels. In this experimental work, we intended to prepare the hybrid metal matrix composites such as aluminum alloy 7079 with reinforcement of $ZrO_2 + Si_3N_4$ through stir-casting process. Major findings of this work, as to optimize the stir-casting process, can be to continually conduct wear test and evaluate the microhardness of the stir-casted specimens. Optimization of stir-casting process parameters is a preliminary work for this research by Taguchi tool. The chosen parameters are % of reinforcement (0%, 4%, 8%, and 12%), agitation speed (450 rpm, 500 rpm, 550 rpm, and 600 rpm), agitation time (15 min, 20 min. 25 min, and 30 min), and molten temperature (700°C, 750°C, 800°C, and 850°C). The prepared stir-casted materials are tested by wear analysis and microhardness analysis, through Pin-on-Disc wear tester and Vickers hardness tester, respectively. Wear parameters are optimized, the minimum wear rate is evaluated, and also the wear worn-out surfaces are examined through SEM analysis.

1. Introduction

Aluminum alloys provide excellent mechanical properties for all types fabrication process, as well as machinability characteristics; further, its strength can be increased by adding reinforcement particles. Addition of hard ceramic particles offers good strength of the alloy materials and also enhances the mechanical properties.

Wang et al. [1] investigated the tribological and mechanical strength of the magnesium matrix composites; they prepared the AZ91 magnesium ally with accumulation of graphite particles. Graphite is added at 5%, 10% of volume fraction levels to the magnesium alloy, and compared to both levels of volume fraction, the 10% reduces the wear rate. On the contrary, 10% of graphite can decrease the mechanical strength such as yield strength, tensile strength, and elongation. In the base alloy using 5% of graphite, it can be simply refined well in condition and form a uniform mixture.

Fenghong et al. [2] prepared the aluminum hybrid metal matrix composites with the addition of silicon carbide and tungsten carbide using stir-casting process. The authors are evaluating the mechanical strength and wear properties of the composites in a detailed experimental work. In the microstructural study, silicon carbide and tungsten carbide particles are mixed in an unvarying manner into the

aluminum alloy material. Higher hardness values are examined in all measurements due to extreme merger of the reinforcement particles to the base materials. Wear resistance of the composites is enormously increased for the massive fusion of the hard particles in the stir-casting process.

Palanikumar et al. [3] carried out the wear analysis of aluminum alloy 6061 with addition of boron carbide and mica material; the composites are synthesized by stir-casting process. They conducted the wear test to examine the wear rate, as well as coefficient of friction of the stir-casted composite specimens. In the friction stir-casting process, the 70 μm of boron carbide particles and 10 μm of mica particles are added. For their investigations, the parameters of dry sliding wear test are chosen as applied load of 10 N, 20 N, and 30 N. Finally, the better wear reduction rate and coefficient of friction were obtained in the AA6061/B_4C/Mica composites in contrast with AA6061/B_4C composites.

Singh and Chauhan [4] investigated the wear performance of the aluminum matrix composites, namely, aluminum alloy together with silicon carbide and red mud prepared by stir-casting method. Statistical approach (Taguchi) is involved for their investigations, and parameters are preferred as percentage of red mud fraction, particle size and applied load, sliding distance, and sliding velocity. In their analysis, the sliding distance has chief parameter of influence in the wear loss examination; similarly, the applied load has extreme role of coefficient friction analysis. For this analysis, enhanced wear resistance was obtained through increasing level of red mud percentage and decrease of load and sliding distance.

Kurapati et al. [5] conducted the wear study of the aluminum alloy 2024 with added different percentage level of fly ash and silicon carbide. Reinforcement percentage of the fly ash and silicon carbide is taken in equivalent weight fraction with different percentage levels (5%, 10%, and 15%). The authors considered L27 orthogonal arrays for their investigation. Wear resistance of the composites is increased by the increase of applied load and sliding distance. Among the three parameters, the applied load was the higher influencing factor on the wear test compared to other factors such as sliding time and percentage of reinforcement.

Stir-casting process was highly involved to enhance the mechanical properties and strengthening of different alloy materials for reinforcement of hared particles [6–8]. Process parameters of the stir-casting method have a powerful role in the composite preparation, and each parameter is involved on its own characters [3, 9–11]. Combined parameters are modifying the result of the composites. Wear analysis has an extremely important role in the alloy materials to find the wear resistance. Generally, the wear test is conducted in either dry or wet conditions. In the wear test, important parts are to be considered such as weight loss, frictional force worn-out surfaces, and coefficient of friction [12–14]. Microhardness test involves measuring the hardness of the materials effectively and precisely. Compared to other hardness tests, the Vickers hardness test is the best suited method to measure the hardness, because the accuracy of testing and damage of the specimen is less [15–18]. In this research, linked to all factors and deep study of literature, the aluminum metal matrix composites are chosen. For this experimental work, we considered the base material as aluminum alloy 7079 with reinforced particles of zirconium oxide (ZrO_2) and silicon nitride (Si_3N_4). Hybrid composites are prepared through stir-casting process, and the process parameters of the stir-casting are optimized by Taguchi route [19]. The main objectives of this work are to find the mechanical and tribological characteristics of the AMMC's for analysis of compaction characteristics of the powders. Hence, the stir-casted composites are tested by Pin-On-Disc apparatus for estimating of wear rate; further, the Vickers microhardness is used to measure the hardness value of the stir-casted part [20–22].

2. Materials

X-ray Fluorescence (XRF) technique was used to measure the elemental composition of the aluminum alloy material (AA7079).

Aluminum alloy 7079 material was selected for this study due to high corrosion resistance, extreme strength, better ductility, and excellent thermal and electrical properties [23–25]. These alloys are originally in wrought alloy, and it has extreme machinability nature. Highly stressed components used in the machineries, mobile industry apparatus, hydraulic valves manufacturing, and air wings parts are fabricated by AA7079 alloy. Zirconium oxide and silicon nitride particles are chosen as reinforced particles of this study. Exceptional strength of the reinforced particles is added to base material, and it can increase the strength of the base material [26–28]. Table 1 presents the chemical elements presents in the base material such as aluminum alloy AA7079.

3. Experimental Procedure

In the initial stage, the aluminum alloy and reinforced particles are stir-casted by using stir-casting process, and the process is to be controlled by influencing various process parameters. Further, the wear test and microhardness test are to be conducted [29–31]. Table 2 presents the different parameters and their levels of the stir-casting process. The L16 OA was executed; four parameters are used to cast the aluminum metal matrix hybrid composites, namely, % of reinforcement, agitation speed (rpm), agitation time (min), and molten temperature (^oC).

Figure 1 illustrates the stir-casting process equipment and the setup. In this work, liquid state stir-casting is selected for obtaining homogeneous mixture of base materials and reinforced particles. AA7079 plates are sliced into small sizes and put into the 5 kg capacity of the crucible; further, the crucible is placed inside of the stir-casting machine [32–34]. Heating up the crucible using different temperature levels (700°C, 750°C, 800°C, and 850°C) is done up to melting the aluminum alloy. At the same time, the reinforced particles (zirconium oxide and silicon nitride) are preheated in the muffle furnace using of crucible, and both particles are taken with the same weight ratio but different percentage

Table 1: Chemical opus of aluminum alloy (AA7079).

Material	% of composition
Cr	0.2
Cu	0.5
Fe	0.2
Mg	3.5
Mn	0.24
Si	0.25
Zn	4.0
Ti	0.7
Al	Remaining

Table 2: Stir-casting process parameters and its levels.

S. no.	Parameters	Level 1	Level 2	Level 3	Level 4
1.	% of reinforcement	0	4	8	12
2.	Agitation speed (rpm)	450	500	550	600
3.	Agitation time (min)	15	20	25	30
4.	Molten temperature (°C)	700	750	800	850

Figure 1: Stir-casting process equipment and setup.

levels [35]. Further, both base material and reinforced particles are mixed well in the stir-casting machine with the aid of stirrer and various agitation speeds (450 rpm, 500 rpm, 550 rpm, and 600 rpm). Different agitation time periods (15 min, 20 min, 25 min, and 30 min) were maintained to obtain the homogeneous mixture of the composites. Finally, the molten material in the crucible was poured in the die for required shapes.

3.1. Wear Test. Constant levels of parameters are used to stir-casting the wear test specimens such as 8% of reinforcement, 600 rpm of agitation speed, 30 min of agitation time, and 850°C of molten temperature [36]. Table 3 presents the wear test parameters and its levels, and the parameters are, namely, % of reinforcement, applied load (N), disc speed (m/s), and sliding distance (m). All the parameters are having different set of value levels.

Wear test was conducted in the Pin-On-Disc apparatus for the model of DUCOM, and the wear of the specimens is

Table 3: Wear test process parameters and their levels.

S. no,	Parameters	Level 1	Level 2	Level 3	Level 4
1.	% of reinforcement	0	4	8	12
2.	Applied load (N)	15	25	35	45
3.	Disc speed (m/s)	1.0	1.5	2.0	2.5
4.	Sliding distance (m)	1000	1200	1400	1600

tested by dry sliding mode. The dry sliding wear test apparatus was illustrated in Figure 2, and different loads were applied based on the parameter involvement. All sixteen specimens are wear-tested as per the American Society of Testing Materials (ASTM G99) standard procedure, and the dimensions of the specimen were 40 mm in length and 12 mm in diameter.

Each specimen was tested by using different parameters based on the L16 Orthogonal Array arrangement. Figure 3 illustrates the wear test specimen of the 16 numbers.

3.2. Vickers Microhardness Test. Vickers microhardness testing is one of the optical measurement arrangements. The specimens are prepared as per the ASTM E-384 standards. The diamond indenter was used to measure the hardness value of the specimens by applying little amount of load, and the indentation was made on the surface of the specimen. Normally, the load variation in the Vickers hardness test is 10 gm to 1 kgf, and for this test, the 0.5 kgf load was applied. Figure 4 presents the microhardness test specimen of this experimental work.

4. Results and Discussion

4.1. Wear Test. Table 4 presents the experimental summary of wear test, and the minimum wear rate was obtained as 0.228 mm^3/m for the contribution of 12% of reinforcement, 25 N of applied load, 2 m/s of disc speed, and 1000 m of sliding speed.

Table 5 presents the response table for means of wear test, and Table 6 presents the response table for S/N ratios of the wear test. All the input values are changed into mean and S/N ratio values of the wear test through Design of Experiments. From the wear test, the % of reinforcement was the extremely influenced parameter for effects in the wear test followed by sliding distance, applied load, and disc speed. The optimal parameter of the wear test was recorded as 12% of reinforcement, 25 N of applied load, 1.5 m/s of disc speed, and 1000 m of sliding speed.

Figures 5 and 6 illustrate the main effects plot for mean and S/N ratios of the wear test. Without reinforcement, the specimen was highly affected from the wear; hence, the wear rate was more. Further, increasing reinforcement percentage, the wear rate was reduced. At last, the higher percentage of reinforcement (12%) offered minimum wear rate. In applied load condition, initially, the wear rate was high in lower applied load; further, increasing applied load (25 N), the wear rate can be reduced suddenly. Once again, increasing applied load from 25 N to 45 N, the wear rate was increased. In disc speed condition, 1.5 m/s offered minimum level of wear rate; further, increasing disc speed, the wear

Figure 2: Stir-casting process equipment and setup.

Figure 3: Image of wear test specimens.

Figure 4: Image of Vickers microhardness test specimens.

rate also increased. For the sliding distance condition, the minimum level of sliding speed (1000 rpm) is recorded as lower wear rate, and continually increasing sliding distance, the wear rate was increased.

Figure 7 demonstrates the residual plots for wear rate. In the residual plot, all four graphs explain the parameters influence in single view. In normal probability plot, all sixteen points touch the probability line, with few of them nearer to the line, and it can be reflected in the result of the wear rate, as conducted experimental runs were precise. In the fits plot, the points were scattered uniformly, and within the limits, this can register the selected parameters, and the response values are accurate. From the histogram plot, the all rectangle boxes are extremely close to each other. In the order plot, the points crossed the mean line both positively and negatively simultaneously. From these conditions, the experiment was conducted in an excellent way, and usage of the parameters was effective.

Figure 8 illustrates the experimental runs versus wear rate of the wear test. From the wear test, the experimental and predicted values are analyzed. In sixteen experimental runs, most of the experimental values are within the limit of predicted values; few were nearer and crossed the predicted values.

Figures 9(a)–9(c) illustrates the surface plot of the wear test. Figure 9(a) demonstrates the % of reinforcement versus the applied load. From this plot, the minimum wear was registered as the influence of minimum level of applied load and maximum level of reinforcement. Figure 9(b) presents the applied load versus the disc speed. In this plot, the maximum level of applied load and minimum level of disc speed offered minimum wear rate. Figure 9(c) exemplifies the disc speed versus the sliding distance. From this plot, the moderate level of disc speed and the minimum sliding distance offered minimum wear rate. Figure 9(d) represents the sliding distance versus the % of reinforcement. In this plot, the minimum sliding distance and maximum reinforcement percentage offered lower wear rate.

Figures 10(a)–10(p) illustrate the 3D Profilometric images of the wear specimens in sixteen numbers. These images were converted from the SEM images, and the colors simply identified the wear worn-out surfaces. Blue with white color represents the microns level of wear that can take place, the green color illustrates the moderate level of wear that took place, and finally the red color noticed that the high wear occurred on the surface of the specimens. In the color bar range of wear was marked in microns level. Figure 10(g) shows the minimum wear, Figures 10(h)–10(j) and 10(o) show the moderate wear, and Figures 10(a), 10(b), 10(d), and 10(k) show the high wear.

4.2. Vickers Microhardness Test. Table 7 illustrates the experimental summary of Vickers microhardness test, and the maximum hardness was recorded as 122 VHN. The maximum hardness values were obtained by the influence of the parameters 12% of reinforcement, agitation speed of 450 rpm, agitation time of 30 min, and molten temperature of 750°C.

Table 8 presents the response table for means of Vickers hardness test, and Table 9 presents the response table for S/N ratios of the Vickers hardness test. For these tables, all the input values are converted into mean and S/N ratio values of the Vickers hardness test through Design of Experiments. In the Vickers hardness test, the % of reinforcement was the

Table 4: Experimental summary of wear test.

Exp. runs	% of reinforcement	Applied load (N)	Disc speed (m/s)	Sliding distance (m)	Wear rate (mm^3/m)
1	0	15	1.0	1000	0.572
2	0	25	1.5	1200	0.379
3	0	35	2.0	1400	0.792
4	0	45	2.5	1600	0.823
5	4	15	1.5	1400	0.548
6	4	25	1.0	1600	0.697
7	4	35	2.5	1000	0.418
8	4	45	2.0	1200	0.815
9	8	15	2.0	1600	0.734
10	8	25	2.5	1400	0.483
11	8	35	1.0	1200	0.392
12	8	45	1.5	1000	0.582
13	12	15	2.5	1200	0.676
14	12	25	2.0	1000	0.228
15	12	35	1.5	1600	0.346
16	12	45	1.0	1400	0.286

Table 5: Response table for means (wear test)

Level	% of reinforcement	Applied load (N)	Disc speed (m/s)	Sliding distance (°C)
1	0.6415	0.6325	0.4868	**0.4500**
2	0.6195	**0.4468**	**0.4638**	0.5655
3	0.6477	0.4870	0.6423	0.5273
4	**0.3840**	0.6265	0.6000	0.6500
Delta	0.2575	0.1858	0.1785	0.2000
Rank	1	3	4	2

Table 6: Response table for signal to noise ratios (wear test)—smaller is better.

Level	% of reinforcement	Applied load (N)	Disc speed (m/s)	Sliding distance (°C)
1	4.249	4.041	6.749	**7.493**
2	4.428	**7.681**	**6.893**	5.435
3	5.461	6.739	4.832	6.111
4	**9.083**	4.761	4.748	4.183
Delta	4.834	3.640	2.145	3.310
Rank	1	3	4	2

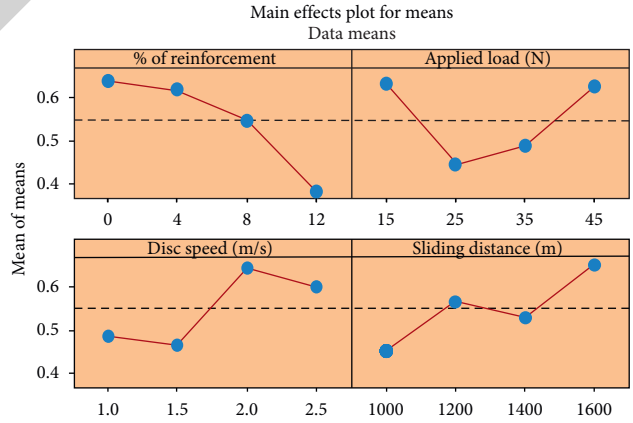

Figure 5: Main effects plot for means (wear test).

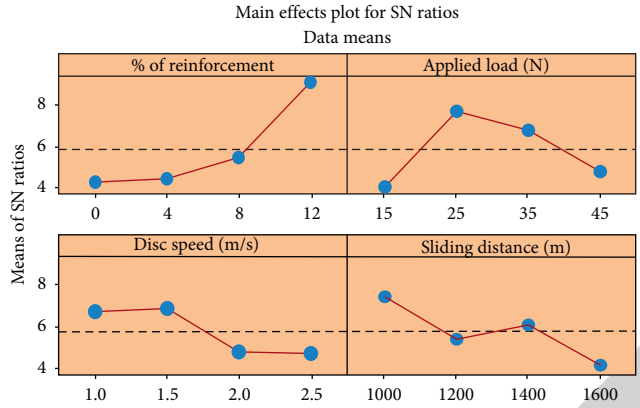

Figure 6: Main effects plot for S/N ratios (wear test).

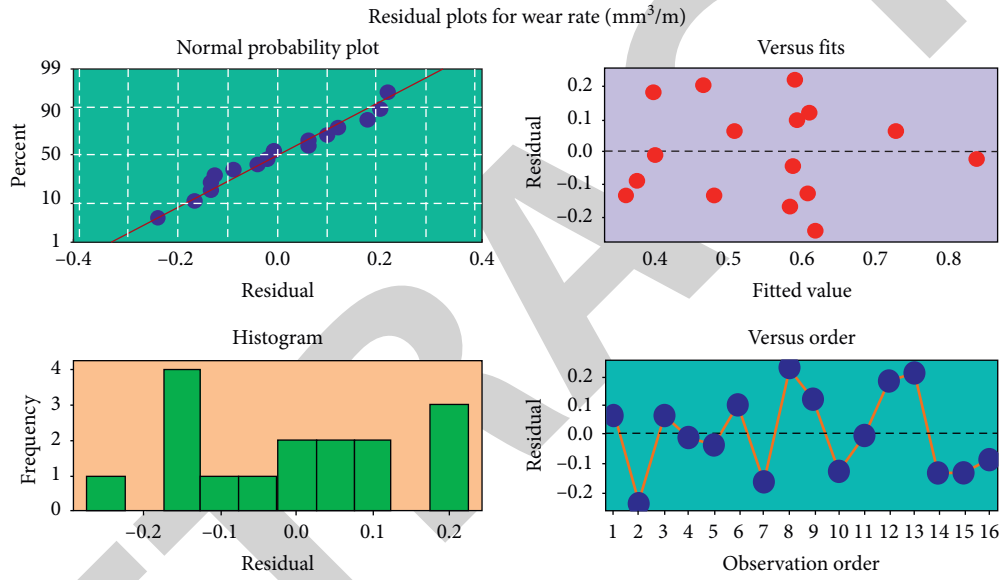

Figure 7: Residual plots for wear rate.

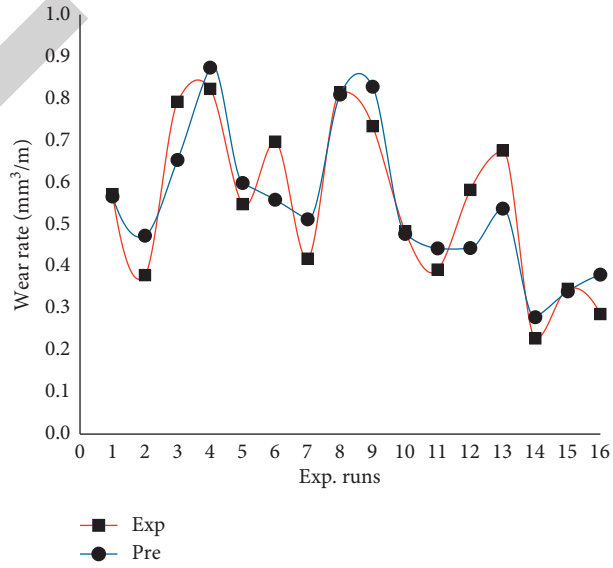

Figure 8: Experimental runs versus wear rate.

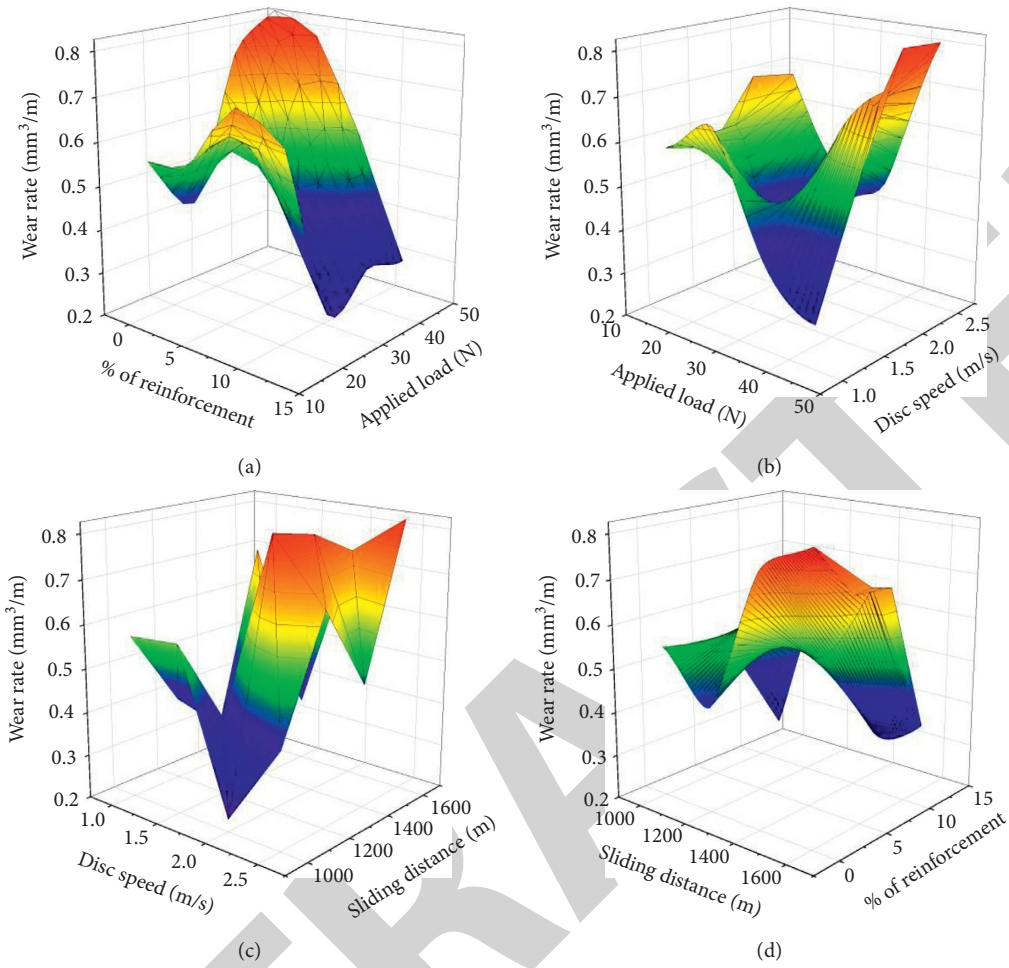

Figure 9: (a) % of reinforcement versus the applied load. (b) Applied load versus the disc speed. (c) Disc speed versus the sliding distance. (d) Sliding distance versus % of reinforcement.

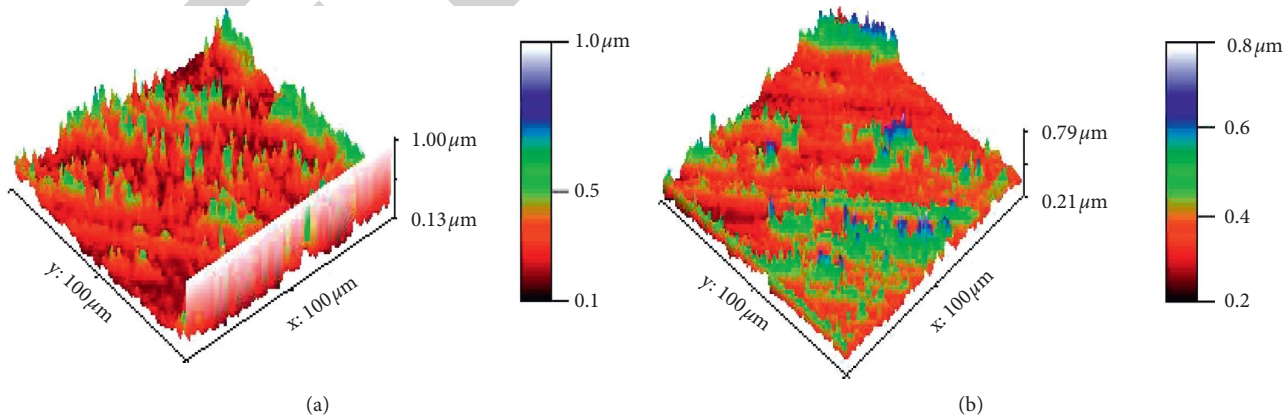

Figure 10: Continued.

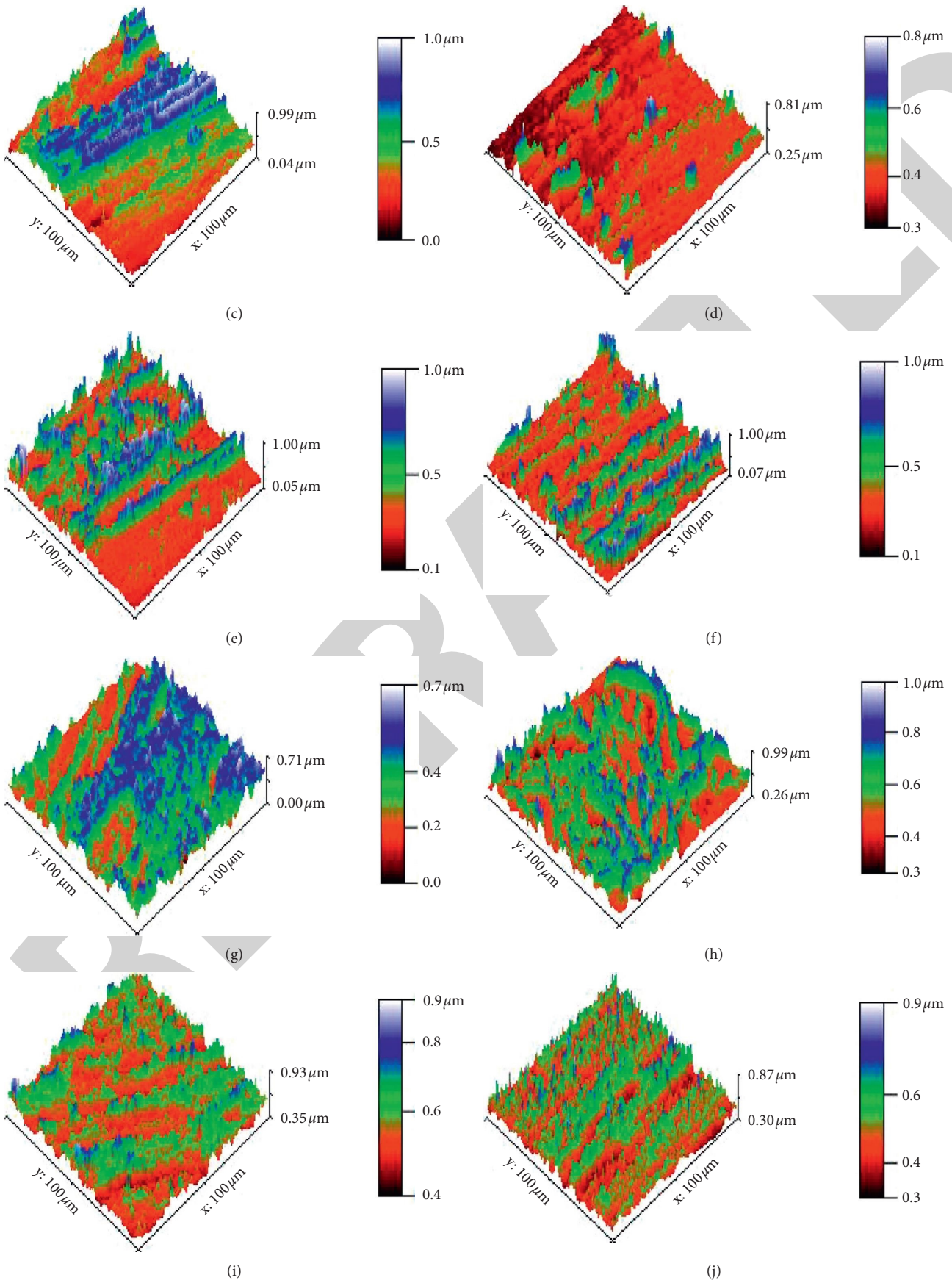

Figure 10: Continued.

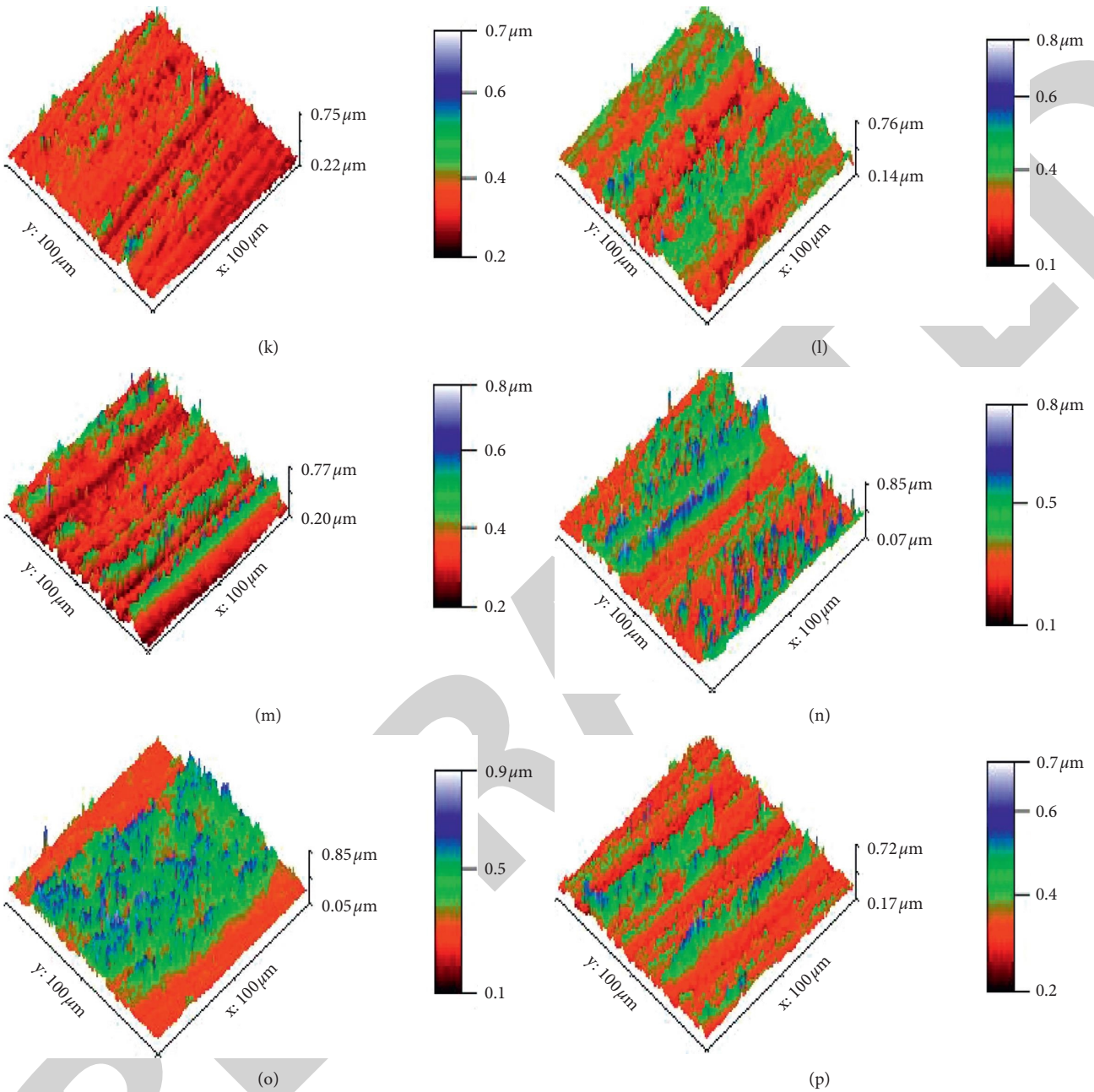

Figure 10: 3D Profilometric images: (a) (S-1). (b) (S-2). (c) (S-3). (d) (S-4). (e) (S-5). (f) (S-6). (g) (S-7). (h) (S-8). (i) (S-9). (j) (S-10). (k) (S-11). (l) (S-12). (m) (S-13). (n) (S-14). (o) (S-15). (p) (S-16).

Table 7: Experimental summary of Vickers hardness test.

Exp. runs	% of reinforcement	Agitation speed (rpm)	Agitation time (min)	Molten temperature (°C)	Vickers hardness (VHN)
1	0	450	15	700	107
2	0	500	20	750	99
3	0	550	25	800	112
4	0	600	30	850	110
5	4	450	20	800	114
6	4	500	15	850	108
7	4	550	30	700	115
8	4	600	25	750	118

Table 7: Continued.

Exp. runs	% of reinforcement	Agitation speed (rpm)	Agitation time (min)	Molten temperature (°C)	Vickers hardness (VHN)
9	8	450	25	850	120
10	8	500	30	800	121
11	8	550	15	750	117
12	8	600	20	700	113
13	12	450	30	750	122
14	12	500	25	700	116
15	12	550	20	850	121
16	12	600	15	800	115

Table 8: Response table for means (Vickers hardness test).

Level	% of reinforcement	Agitation speed (rpm)	Agitation time (min)	Molten temperature (°C)
1	107.0	115.8	111.8	112.8
2	113.8	111.0	111.8	114.0
3	117.8	**116.3**	116.5	**115.5**
4	**118.5**	114.0	**117.0**	114.8
Delta	11.5	5.3	5.3	2.8
Rank	1	2	3	4

Table 9: Response table for signal to noise ratios (Vickers hardness test); larger is better.

Level	% of reinforcement	Agitation speed (rpm)	Agitation time (min)	Molten temperature (°C)
1	40.58	41.26	40.96	41.06
2	41.11	40.88	40.94	41.11
3	41.42	**41.30**	41.32	**41.25**
4	**41.47**	41.14	**41.36**	41.18
Delta	0.89	0.42	0.41	0.21
Rank	1	2	3	4

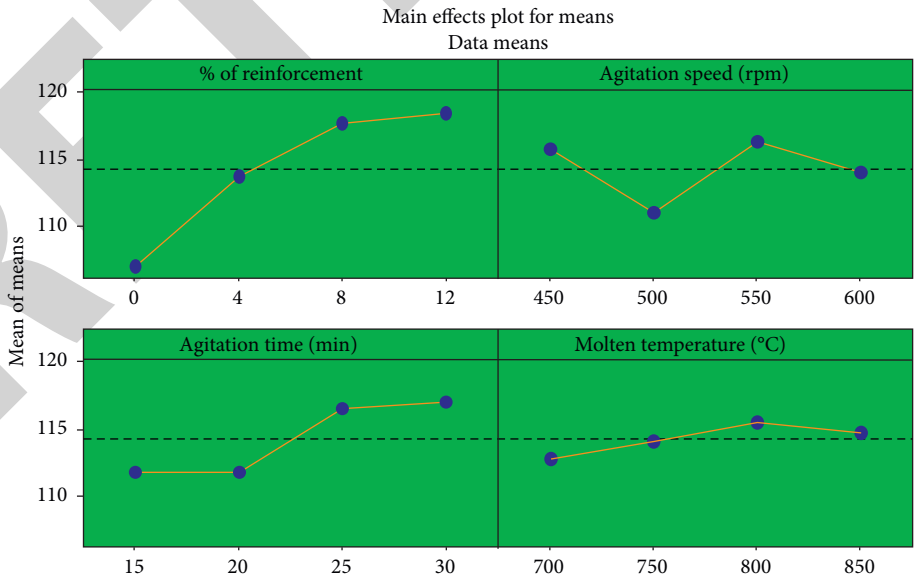

Figure 11: Main effects plot for means (Vickers hardness test).

particularly influenced parameter for effects in the Vickers hardness test continued by agitation speed, agitation time, and molten temperature. Optimal parameter of the Vickers hardness test was found as 12% of reinforcement, 550 rpm of agitation speed, 30 min of agitation time, and 800°C of molten temperature.

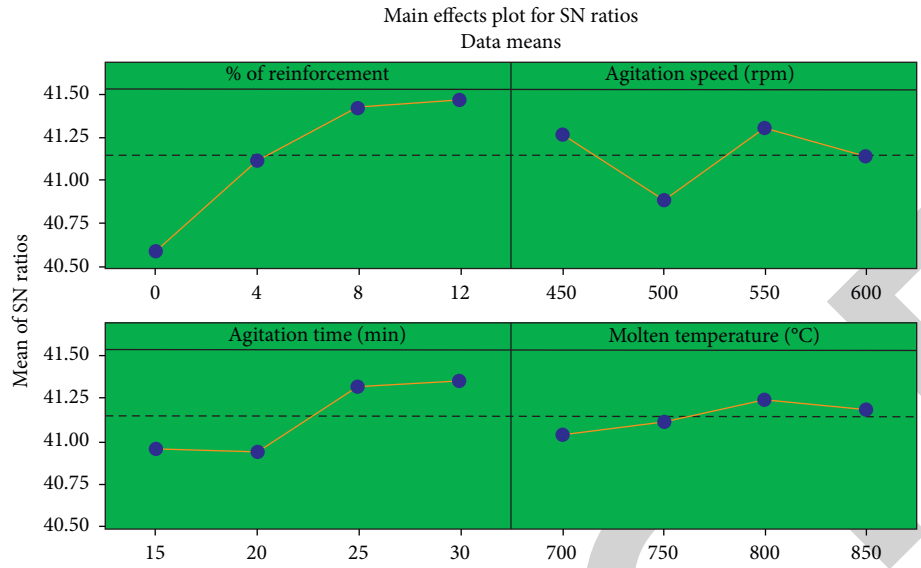

Figure 12: Main Effects plot for S/N ratios (Vickers hardness test).

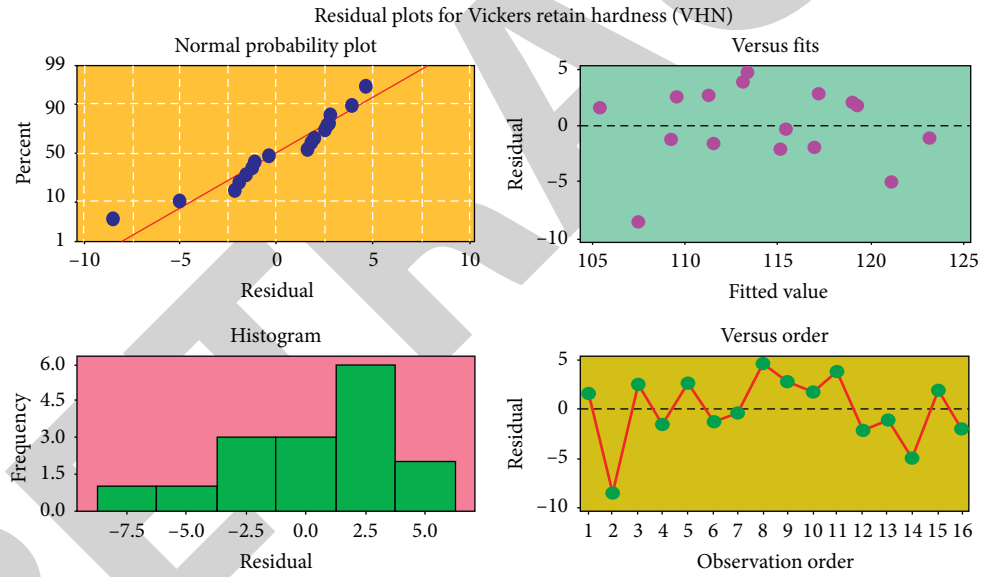

Figure 13: Residual plots for Vickers hardness.

Figures 11 and 12 exemplify the main effects plot for mean and S/N ratios of the Vickers hardness test. Increasing reinforcement percentage, the microhardness value was increased. Finally, the higher percentage of reinforcement (12%) provided maximum microhardness. In agitation speed state, initially, the microhardness was high in lower agitation speed; further, increasing agitation speed (500 rpm), the microhardness value was reduced suddenly. Increasing agitation speed from 500 rpm to 550 rpm, the microhardness was increased. In agitation time state, increasing gradually the agitation time, the microhardness value was increased; 30 min of agitation time provided the maximum hardness values. For the molten temperature condition, the minimum level of molten temperature was registered as lower microhardness, and constantly increasing molten temperature, the microhardness increased. Finally, the 800°C offered maximum microhardness values.

Figure 13 displays the residual plots for Vickers hardness. In the residual plot, the microhardness level and the parameters influence are clearly exemplified in single observation. For the normal probability plot, all sixteen points are lying on the probability line few of them nearer to the line, and it can be replicated in the effect of the microhardness such as carrying out experimental runs. In the fits plot, the points were distributed unvaryingly, and within the limits, the chosen parameters can be recorded, and the response values are perfect. From the histogram plot, all rectangle boxes are extremely close and touch each other. in

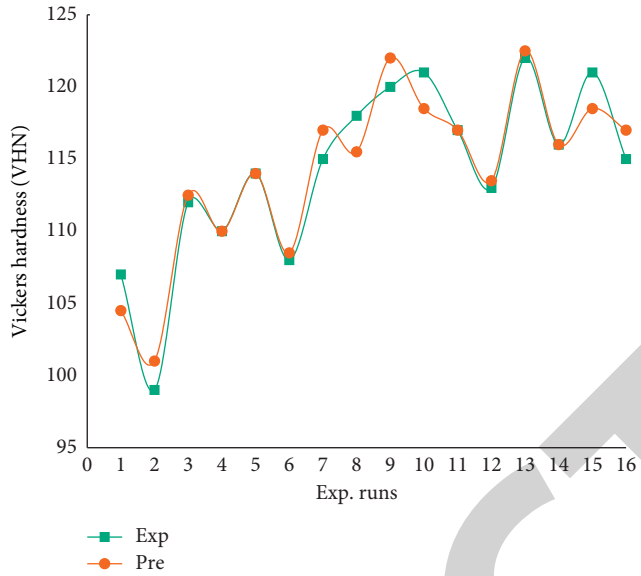

Figure 14: Experimental runs versus Vickers microhardness.

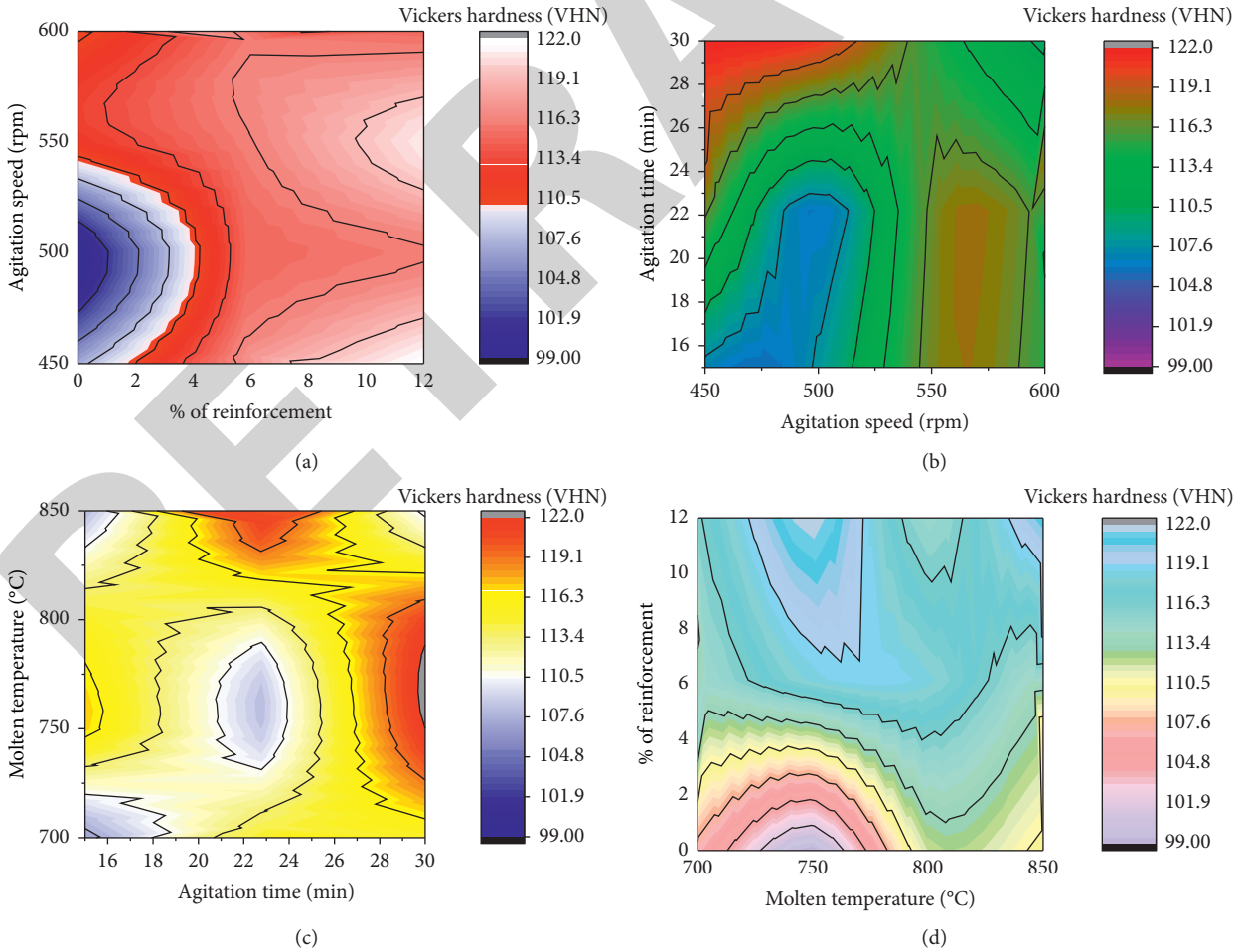

Figure 15: (a) Contour plot: % of reinforcement. (b) Contour plot: agitation speed. (c) Contour plot: agitation speed. (d) Contour plot: molten temperature versus % of reinforcement.

the order plot, all points crossed simultaneously the mean line both positively and negatively. From these conditions, the experiment carried out was done in an exceptional manner, and using the parameters was efficient.

Figure 14 illustrates the experimental runs versus Vickers microhardness. From the Vickers microhardness test, the experimental and predicted values are evaluated. In the sixteen experimental runs, the majority of the experimental values are within the limit of the predicted values; few were nearer and crossed the predicted values.

Figures 15(a)–15(d) present the contour plot of the Vickers microhardness test. Figure 15(a) shows the correlation between % of reinforcement and agitation speed, and the higher reinforcement percentage and moderate agitation speed offered excellent microhardness. Figure 15(b) illustrates the connection between agitation speed and agitation time, and the minimum agitation speed and higher agitation time provided maximum hardness value. Figure 15(c) demonstrates the relationship between agitation time and molten temperature, and the maximum agitation time and moderate molten temperature were recorded as maximum hardness value.

Figure 15(d) reveals the correlation between molten temperature and % of reinforcement, and the moderate molten temperature and higher reinforcement were registered as maximum hardness value.

5. Conclusions

Aluminum alloy 7079 with the addition of zirconium oxide and silicon nitride (AMCs) hybrid composites was prepared through stir-casting process. Further, the wear test was conducted by Pin-On-Disc with Taguchi statistical approach. Finally, the wear worn-out surfaces and Vickers microhardness were examined thoroughly. The output result of this experimental work was concluded and demonstrated as follows:

(i) From the wear test, the minimum wear rate was recorded as 0.228 mm^3/m, the contribution of reinforcement 12%, applied load 25 N, disc speed 2 m/s and sliding speed 1000 m, which offered minimum wear rate. In the wear test, the % of reinforcement was the exceptionally influenced parameter for effects in the wear test followed by sliding distance, applied load, and disc speed. Optimal parameter of the wear test was registered as 12% of reinforcement, 25 N of applied load, 1.5 m/s of disc speed, and 1000 m of sliding speed.

(ii) In the surface plot analysis, the minimum level of applied load and maximum level of reinforcement offered minimum wear rate. Further, the maximum level of applied load and minimum level of disc speed offered minimum wear rate. Correlation between two parameters, the minimum sliding distance and maximum reinforcement percentage, offered lower wear rate.

(iii) For the Vickers microhardness test, the maximum hardness was recorded as 122 VHN. The maximum hardness values were obtained by the influence of the parameters, which are 12% of reinforcement, agitation speed of 450 rpm, agitation time of 30 min, and molten temperature of 750°C. In the Vickers hardness test, the % of reinforcement was the predominantly influenced parameter for effects in the Vickers hardness test, followed by agitation speed, agitation time, and molten temperature. Optimal parameter of the Vickers hardness test was recorded as 12% of reinforcement, 550 rpm of agitation speed, 30 min of agitation time, and 800°C of molten temperature.

(iv) From the contour plot analysis, the higher reinforcement percentage and moderate agitation speed offered exceptional microhardness. Further, the minimum agitation speed and higher agitation time presented the maximum hardness value. Finally, the maximum agitation time and moderate molten temperature were recorded as maximum hardness value.

Data Availability

The data used to support the findings of this study are included within the article. Should further data or information be required, these are available from the corresponding author upon request.

Disclosure

This study was performed as a part of the Employment of College of Engineering and Technology, Dambi Dollo University, Oromia Region, Ethiopia.

Conflicts of Interest

The authors declare that there are no conflicts of interest regarding the publication of this paper.

Acknowledgments

The authors appreciate the supports from Dambi Dollo University, Ethiopia, and Sathyabama Institute of Science and Technology, Chennai. The authors thank Saveetha School of Engineering, Chennai, for the technical assistance in the design of experiment process.

References

[1] C.-R. Wang, K.-K. Deng, and Y. Bai, "Microstructure, and mechanical and wear properties of Grp/AZ91 magnesium matrix composites," *Materials*, vol. 12, no. 7, pp. 1190–1206, 2019.

[2] C. Fenghong, C. Chang, W. Zhenyu, T. Muthuramalingam, and G. Anbuchezhiyan, "Effects of silicon carbide and tungsten carbide in aluminium metal matrix composites," *Siliconindia*, vol. 11, no. 6, pp. 2625–2632, 2019.

[3] K. Palanikumar, S. Eaben Rajkumar, and K. Pitchandi, "Influence of primary B_4C particles and secondary mica particles on the wear performance of Al6061/B_4C/mica hybrid

composites," *Journal of Bio and Tribo-Corrosion*, vol. 5, no. 3, Article ID 77, 2019.

[4] J. Singh and A. Chauhan, "Investigations on dry sliding frictional and wear characteristics of SiC and red mud reinforced Al2024 matrix hybrid composites using taguchi's approach," *Proceedings of the Institution of Mechanical Engineers—Part L: Journal of Materials: Design and Applications*, vol. 233, no. 9, pp. 1923–1938, 2018.

[5] V. B. Kurapati, R. Kommineni, and S. Sundarrajan, "Statistical analysis and mathematical modeling of dry sliding wear parameters of 2024 aluminium hybrid composites reinforced with fly ash and SiC particles," *Transactions of the Indian Institute of Metals*, vol. 71, no. 7, pp. 1809–1825, 2018.

[6] S. Koksal, F. Ficici, R. Kayikci, and O. Savas, "Experimental optimization of dry sliding wear behavior of in situ AlB2/Al composite based on Taguchi's method," *Materials and Design*, vol. 42, pp. 124–130, 2012.

[7] L. Natrayan, V. Sivaprakash, and M. S. Santhosh, "Mechanical, microstructure and wear behavior of the material AA6061 reinforced SiC with different leaf ashes using advanced stir casting method," *International Journal of Engineering and Advanced Technology*, vol. 8, pp. 366–371, 2018.

[8] M. Udayakumar, S. Aravindan, and K. Rajkumar, "Wear performance of Al-SiC- B_4C hybrid composites under dry sliding conditions," *Materials and Design*, vol. 47, pp. 456–464, 2013.

[9] R. Pandiyarajan, P. Maran, S. Marimuthu, and K. C. Ganesh, "Mechanical and tribological behavior of the metal matrix composite AA6061/ZrO_2/C," *Journal of Mechanical Science and Technology*, vol. 31, no. 10, pp. 4711–4717, 2017.

[10] J. Singh and A. Chauhan, "Overview of wear performance of aluminium matrix composites reinforced with ceramic materials under the influence of controllable variables," *Ceramics International*, vol. 42, no. 1, pp. 56–81, 2016.

[11] V. Kavimani, K. S. Prakash, T. Thankachan, S. Nagaraja, A. K. Jeevanantham, and J. P. Jhon, "WEDM parameter optimization for silicon@r-GO/magneisum composite using taguchi based GRA coupled PCA," *Siliconindia*, vol. 12, no. 5, pp. 1161–1175, 2020.

[12] D. Bandhu, A. Thakur, R. Purohit, R. K. Verma, and K. Abhishek, "Characterization & evaluation of Al7075 MMCs reinforced with ceramic particulates and influence of age hardening on their tensile behavior," *Journal of Mechanical Science and Technology*, vol. 32, no. 7, pp. 3123–3128, 2018.

[13] M. H. Faisal and S. Prabagaran, "Investigation on mechanical and wear properties of aluminium based metal matrix composite reinforced with B_4C, Gr and fly ash," in *Advanced Manufacturing and Materials Science*, pp. 379–385, Springer, Berlin, Germany, 2018.

[14] R. S. Bhatia and K. Kudlipsingh, "An experimental analysis of aluminium metal matrix composite using Al_2O_3/B_4C/Gr particles," *International Journal of Advanced Research in Computer Science*, vol. 8, no. 4, pp. 83–90, 2017.

[15] P. V. Reddy, P. R. Prasad, D. M. Krishnudu, and E. V. Goud, "An investigation on mechanical and wear characteristics of Al 6063/TiC metal matrix composites using RSM," *Journal of Bio- and Tribo-Corrosion*, vol. 5, no. 4, p. 90, 2019.

[16] A. Prasad Reddy, P. Vamsi Krishna, and R. N. Rao, "Tribological behaviour of Al6061-2SiC-xGr hybrid metal matrix nanocomposites fabricated through ultrasonically assisted stir casting technique," *Siliconindia*, vol. 11, no. 6, pp. 2853–2871, 2019.

[17] S. Suresh, G. H. Gowd, and M. L. S. D. Kumar, "Mechanical and wear characterization of Al/nano-SiC NMMCs by liquid state process," *Journal of Bio- and Tribo-Corrosion*, vol. 5, no. 2, pp. 43–53, 2019.

[18] K. K. Alaneme and K. O. Sanusi, "Microstructural characteristics, mechanical and wear behaviour of aluminium matrix hybrid composites reinforced with alumina, rice husk ash and graphite," *Engineering Science and Technology, an International Journal*, vol. 18, no. 3, pp. 416–422, 2015.

[19] L. Natrayan and M. S. Kumar, "Influence of silicon carbide on tribological behaviour of AA2024/Al_2O_3/SiC/Gr hybrid metal matrix squeeze cast composite using Taguchi technique," *Materials Research Express*, vol. 6, no. 12, Article ID 1265f9, 2020.

[20] S. Aribo, A. Fakorede, O. Ige, and P. Olubambi, "Erosion-corrosion behaviour of aluminum alloy 6063 hybrid composite," *Wear*, vol. 376-377, pp. 608–614, 2017.

[21] K. Hemalatha, C. James, L. Natrayan, and V. Swamynadh, "Analysis of RCC T-beam and prestressed concrete box girder bridges super structure under different span conditions," *Materials Today: Proceedings*, vol. 37, pp. 1507–1516, 2021.

[22] G. Elango, B. K. Raghunath, and K. Palanikumar, "Experimental analysis of the wear behaviour of hybrid metal-matrix composites of LM25Al with equal volumes of SiC+ TiO_2," *Materials Technology*, vol. 48, no. 6, pp. 803–810, 2014.

[23] S. K. Chourasiya, G. Gautam, and D. Singh, "Mechanical and tribological behavior of warm rolled Al-6Si-3Graphite self lubricating composite synthesized by spray forming process," *Siliconindia*, vol. 12, no. 4, pp. 831–842, 2020.

[24] V. Paranthaman, K. Shanmuga Sundaram, and L. Natrayan, "Influence of SiC particles on mechanical and microstructural properties of modified interlock friction stir weld lap joint for automotive grade aluminium alloy," *Silicon*, pp. 1–11, 2021.

[25] S. Banerjee, S. Poria, G. Sutradhar, and P. Sahoo, "Dry sliding tribological behavior of AZ31-WC nano-composites," *Journal of Magnesium and Alloys*, vol. 7, no. 2, pp. 315–327, 2021.

[26] W. Yu, D. Chen, L. Tian, H. Zhao, and X. Wang, "Self-lubricate and anisotropic wear behavior of AZ91D magnesium alloy reinforced with ternary Ti2AlC MAX phases," *Journal of Materials Science & Technology*, vol. 35, no. 3, pp. 275–284, 2019.

[27] T. Sathish and N. Sabarirajan, "Synthesis and optimization of AA 7175—zirconium carbide (ZrC) composites machining parameters," *Journal of New Materials for Electrochemical Systems*, vol. 24, no. 1, pp. 34–37, 2021.

[28] S. E. Rajkumar, K. Palanikumar, and P. Kasiviswanathan, "Influence of mica particles as secondary reinforcement on the mechanical and wear properties of Al/B_4C/mica composites," *Materials Express*, vol. 9, no. 4, pp. 299–309, 2019.

[29] A. Pai, S. S. Sharma, R. E. D'Silva, and R. G. Nikhil, "Effect of graphite and granite dust particulates as micro-fillers on tribological performance of Al 6061-T6 hybrid composites," *Tribology International*, vol. 92, pp. 462–471, 2015.

[30] V. Paranthaman, K. Shanmuga Sundaram, and L. Natrayan, "Effect of silica content on mechanical and microstructure behaviour of resistance spot welded advanced automotive TRIP steels," *Silicon*, Article ID 1, 2021.

[31] K. S. Selvaraj and G. Prabu, "Investigation of the mechanical properties of a squeeze-cast LM6 aluminium alloy reinforced with a zinccoated steel-wire mesh," *Materiali in Tehnologije*, vol. 52, no. 2, pp. 125–131, 2018.

[32] L. Natrayan and M. Senthil Kumar, "An integrated artificial neural network and Taguchi approach to optimize the squeeze cast process parameters of AA6061/Al_2O_3/SiC/Gr hybrid

composites prepared by novel encapsulation feeding technique," *Materials Today Communications*, vol. 25, Article ID 101586, 2020.

[33] S. Ramesh, R. Prabu, and E. Natarajan, "Experimental investigation of structure, wear, and erosion resistance of Ss316 substrate coated with Tic-Al_2O_3 composite by laser cladding," *High Temperature Material Processes An International Quarterly of High-Technology Plasma Processes*, vol. 22, no. 1, pp. 63–71, 2018.

[34] L. Yuan, J. Han, J. Liu, and Z. Jiang, "Mechanical properties and tribological behavior of aluminum matrix composites reinforced with in-situ AlB2 particles," *Tribology International*, vol. 98, pp. 41–47, 2016.

[35] S. J. S. Chelladurai and R. Arthanari, "Effect of stir cast process parameters on wear behaviour of copper coated short steel fibers reinforced LM13 aluminium alloy composites," *Materials Research Express*, vol. 5, no. 6, Article ID 066550, 2018.

[36] Z. Mohamed, A. R. Anwar khan, and P. G. Mukunda, "Evaluation of the Taguchi method for wear behavior of Al6061/CuSiC/Cu-Gr Hybrid composite," *Materials Today: SAVE Proceedings*, vol. 2, no. 4-5, pp. 2951–2958, 2017.